Journal of the Ceramic Society of Japan 116 [10] 1024-1027 2008 Special Article: Review

Interfaces impact on the transmission of chalcogenides photonic crystal fibres

Laurent BRILLAND,† Johan TROLES,* Patrick HOUIZOT,* Frederic DÉSÉVÉDAVY,* Quentin COULOMBIER,* Gills RENVERSEZ, Thierry CHARTIER,*** Thanh Nam NGUYEN,*** Jean-Luc ADAM* and Nicolas TRAYNOR**

PERFOS, Plateforme d'Etudes et de Recherches sur les Fibres Optiques Spéciales, 11 rue Louis de Broglie, 22300 lannion, France
***Equipe Verres et Céramiques, UMR-CNRS 6226, Sciences Chimiques de Rennes, Université de Rennes 1, 35042 Rennes Cedex, France**
****Institut Fresnel, UMR CNRS 6133, Université Aix Marseille, 13397 Marseille, France**
*****Laboratoire Foton, CNRS UMR 6082, ENSSAT, BP 80518, 22305 Lannion Cedex, France**

In this work, we present the fabrication of chalcogenide photonic crystal fibres (PCFs) with a solid core for three different glass composition containing a variety of chalcogens. We show that the Stack and Draw technique currently used for silica PCFs can be problematic in the case of chalcogenides glasses. We prove that excess losses are related to the interface between the capillaries. We also present correct PCF design enables a significant improvement of final fibre losses. We obtained a lowest attenuation of 3 dB/m at 1.55 μm, of 4.5 dB/m at 3.39 μm and 6 dB/m at 9,3 μm.

Key-words : Chalcogenides glasses, Photonic crystal fibres, Optical losses, Infrared fibres

[Received June 6, 2008]

1. Introduction

Chalcogenides glasses are based on chalcogen elements (Sulphur, Selenium and Tellurium) and other additive elements such as Arsenic, Germanium, Antimony, or Gallium. Compared to silica glass, they offer several distinctive optical properties:, their transmission window extends far in the infrared spectral region over the spectral range 0.5–1 μm to 12–18 μm; they exhibit a high level of third order non linear optical susceptibility $\chi^{(3)}$,[1)–4)] which can be two or three orders of magnitude greater than that of silica at 1.55 μm. These properties enable the realisation of a great number of optical devices based on chalcogenide glass fibres. In terms of passive optical functions, laser power transmission,[5),6)] optical sensing,[7)] spatial filtering[8)] and imaging[9)] have already been demonstrated with these fibres. The large non linearity in these fibres gives rise to extremely strong Kerr, Raman or Brillouin effects.[10)–13)] These effects have been successfully used for the generation of active optical functions such as optical signal regeneration, wavelength conversion,[14)] switching[15)] and optical limiting.[16)] Furthermore, several chalcogenide glasses offer the possibility of relatively high concentration rare earth doping for amplification and lasing operations.[17)]

For many applications, the single mode guiding regime is required. The most common single mode fibres are in a core-clad step index configuration. They are realised in general using the reliable double crucible process.[18)] These fibres have been widely used to study optical functions by many research teams. Another kind of fibre offering the possibility of single mode operation is the solid core photonic crystals fibre (PCF).[19)] These fibres exhibit several interesting properties such as endlessly single mode operation, widely tuneable chromatic dispersion, single mode guiding with a large or small effective area. They consist of a periodic lattice of holes arranged around a solid core that run along the fibre length. The distance between hole centres, Λ, the hole diameter d, the number of rings Nr and the index of refraction n, are the main parameters affecting PCF properties. The most common fabrication method is the "Stack and Draw" method that has proven reliable for silica glass for more than a decade.

Recently, chalcogenides PCFs have been fabricated using this technique.[20)–22)] They present important potential for most of the applications note above. One subject of particular interest is the generation of non linear effects in the infrared region by combining the large chalcogenide non linearity with a small guiding mode propagating in PCF. The generation of a spectrally broadband source has already been demonstrated using these fibres.[23)] However, the guiding losses of chalcogenide PCFs are still too high to realize efficient optical function. They can be two or three order larger than the intrinsic chalcogenides material losses.

In this paper, our investigations deal with three compositions of glasses containing various chalcogens (S, Se and Te). We report PCFs transmission measurements from these three glasses compositions and show that the "Stack & Draw" technique can be problematic in the case of these glasses. We indicate the origin of the main loss generating mechanism and present a correct design which enables a significant improvement of final PCF losses.

This paper is divided into five sections. Section two is concerned with chalcogenide glass fabrication, including a description of the glass synthesis process. Optical transmission curves from three compositions are presented. In section three, we describe the PCF fabrication and show their cross section with an original design. Transmission values are given for different wavelengths. Section four discusses of the origin of losses and

† Corresponding author: L. Brilland; E-mail: Laurent.brilland@univ-rennes1.fr

why a specific design improves the transmission.

2. Fabrication of chalcogenides glasses

Chalcogenides glasses are based on Sulphur, Selenium, Tellurium and the addition of other elements such as arsenic, germanium, antimony, gallium, etc. In our work, we are interested in three compositions including the three chalcogen elements: $Ge_{15}Sb_{20}S_{65}$ (GeSbS), $As_{40}Se_{60}$ (AsSe) and $Te_{20}As_{30}Se_{50}$ (TAS). They have been chosen for their great stability against crystallisation effect. Their principal optical and thermal properties are given in **Table 1**.

The high purity raw materials (5N) used for glass fabrication were placed in a silica tube and pumped under vacuum (10^{-5} mbar). A preliminary thermal treatment under vacuum is necessary to remove some residual pollutants present in the raw materials. Water is removed by heating sulphur at 120°C and oxides are removed by heating As and Se respectively at 290°C and 240°C.

After sealing, the silica tube was progressively heated to around 800°C or 900°C during 12 h in a rocking furnace. The batch was then quenched in water and the glass was annealed at the glass transition temperature T_g. At this process stage, some static and dynamical distillation under vacuum has to be done to obtain high purity glass. Solid particles such as carbon can be removed by static distillation. Dynamical distillation enables the removal of bubbles and volatile compounds such as C-S, water and hydrocarbons. The batch was then placed once again in a rocking furnace, quenched and annealed as during the first process stage. The rod sizes obtained were typically 12 mm* 12 cm. One part of them was then drawn down to 400 μm single index fibre (another part was used to make capillaries tube). These single index fibres were used to determine intrinsic glass losses via the cutback method using a FTIR setup. **Figure 1** show the attenuation curves of the three chalcogenides glasses studied. **Table 2** gives the attenuation for different wavelength. For GeSbS glass, the lowest attenuation is 0.2 dB/m at 5.2 μm while it is 1,3 dB/m at 7 μm for TAS glass and it is 0.3 dB/m at 4 μm for AsSe glass. One can observe specific absorption bands at 4.1 μm and 4.5 μm. They are respectively due to S-H and Se-H bonds. Without purification, their intensity can reach more than 50 dB/m.

Table 1. Optical and Thermal Properties of the GaSbS; TeAsSe and AsSe Glasses

Glass composition (mol%)	Glass transition temperature, T_g (°C)	Drawing Temperature (°C)	Refractive index at 1,55 μm	Refractive index at 3.39 μm	Refractive index at 9.3 μm
$Ge_{15}Sb_{20}S_{65}$ (GeSbS)	250	360	2.30	–	–
$As_{40}Se_{60}$ (AsSe)	185	320	2.83	2.78	–
$Te_{20}As_{30}Se_{50}$ (TAS)	137	250	–	2.93	2.90

Table 2. Chalcogenide Material and PCF Optical Losses

Glass	Wavelength (μm)	Material losses (dB/m)	PCFs optical losses (dB/m) **Interstitials holes collapsed**	PCFs optical losses **Interstitials holes opened**
$Ge_{15}Sb_{20}S_{65}$ (GeSbS)	1.55	0.5+/–0.2	> 20	3+/–0.25
	3.39	0.6+/–0.2	> 20	4.5+/–0.25
$As_{40}Se_{60}$ (AsSe)	1.55	1.05+/–0.2	> 20	5+/–0.5
$Te_{20}As_{30}Se_{50}$ (TAS)	3.39	2.5+/–0.2	> 20	9+/–0.5
	9.3	1.5+/–0.2	> 20	6+/–0.5

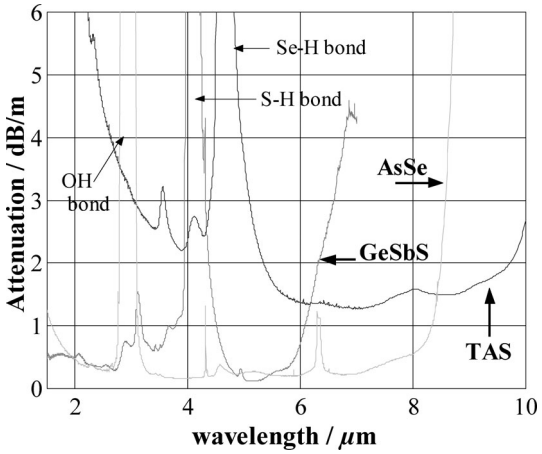

Fig. 1. Attenuation curve of single index GeSbS, AsSe and TeASSe fibres.

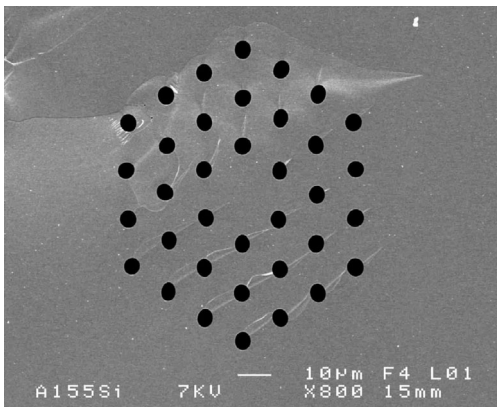

Fig. 2. Cross section of GeSbS photonic crystal fibre: interstitials holes collapsed. Attenuation at 1,55 and 3,39 μm > 20 dB/m.

3. Chalcogenide photonics crystals fibre fabrication and transmission measurements

Chalcogenides glass tubes of 12 mm outside diameter, 5 mm inside diameter and 12 cm length were obtained by a centrifugation technique. Chalcogenide glass placed in a sealed silica ampoule was heated to liquid temperature (typically 700°C). The melt was then spun at around 3000 rpm at ambient temperature during several minutes. After few minutes the vitrified tubes were formed.

One of these tubes was drawn down to obtain capillaries of around 600 μm outside diameter. These were then stacked in a hexagonal lattice around a central rod of identical diameter and placed in a larger jacket tube. The fibre pre-form was realised by applying a depression to perfectly collapse the jacket tube around the microstructure via a descent of a few mm/min in the furnace of the drawing tower. An important point is to adjust parameters of depression and furnace temperature in order to prevent the collapse of capillaries holes and interstitials holes between capillaries. Three pre-forms were been realized, each of them corresponding to one of the glass composition studied.

During the fibre drawing process, two independent variable He gas pressure (or depression) systems were used. One of them maintained pressure inside capillaries holes to prevent their col-

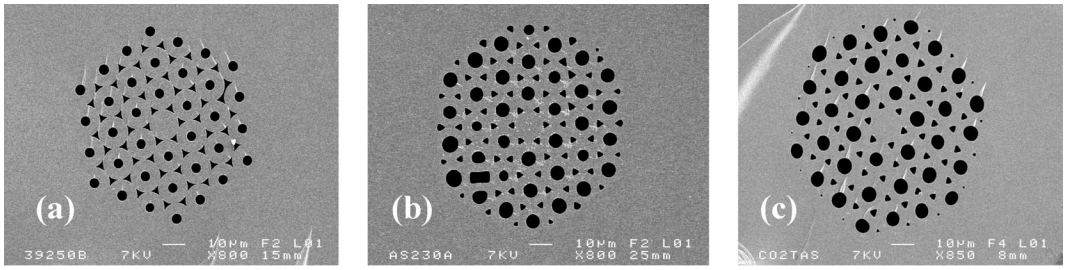

GeSbS AsSe TAS

Fig. 3. Cross sections of chalcogenides photonic crystals fibers ((a) GaSbS, (b) AsSe, (c) TAS): interstitials holes opened.

Table 3. Photonic Crystal Fibre Parameters

Glass	Λ (μm)	d (μm)	d/Λ	r (μm)
$Ge_{15}Sb_{20}S_{65}$ (GeSbS)	13.25+/–0.1	4.19+/–0.05	0.316	3.6
$As_{40}Se_{60}$ (AsSe)	13.35+/–0.1	5.85+/–0.05	0.438	3.55
$Te_{20}As_{30}Se_{50}$ (TAS)	13.77+/–0.1	6.14+/–0.05	0.446	2.92

lapse. The other was applied alternatively in a negative or positive pressure regime inside the interstitial holes. The goal was to obtain sections with open or closed interstitial holes and compare transmission properties. For the three preforms, sections of several meters with interstitials holes collapsed were firstly drawn and secondly section with interstitials holes opened.

Figure 2 shows SEM pictures of the central region of a three rings GeSbS PCF where interstitial holes were collapsed under about 100 mbar of depression while 20 mbar of positive pressure was used in maintaining in capillaries holes. The distance between the hole centers is Λ = 13.25 μm and the hole diameter d is 4.19 μm. Two further three rings AsSe and TAS PCFs (not presented here) with interstitials holes either opened or closed were realised with conditions of pressure and depression close to the same parameters mentioned above. **Figures 3** represent the PCF cross sections of the three chalcogenide glasses studied with a positive pressure (about 10 mbar) applied to open the interstitials holes. The interstitial holes have a triangular form: we define r as the base of an equilateral triangle having an area equal to the area measured by numerical imaging software. **Table 3** gives, for the three PCFs, the average of the geometrical parameters, Λ, d and r taken in the first central ring of holes.

These fibres exhibit single mode operation behaviour for section longer than 20 cm. The output mode profiles were imaged onto infrared cameras using a near field technique for the wavelengths indicated in Table 2. For all sections, the output profiles were accurately fitted with a Gaussian function indicating single mode behaviour. Moreover, by changing injection conditions, no higher order modes were observed. As can be seen in reference,[22] the high refractive index of chalcogenide glass ensures a much stronger confinement than that of silica. Consequently, fewer rings of holes are needed to obtain the same guiding losses. For the d/Λ values given Table 3, three rings of holes ensure guiding losses below the intrinsic material losses given in Table 2.

The attenuation coefficient of both the section with collapsed interstitial holes and the section with opened interstitial holes was then measured for different wavelengths using the cut back method. Sources used for 1.5 μm, 3.39 μm and 9.3 μm are respectively a laser diode connected to a single mode fibre, a CW HeNe laser and a CW CO_2 laser. Detectors used for 1.5 μm, 3.39 μm and 9.3 μm are respectively a photodiode, a non cooled pre-amplified InSb photodiode and a nitrogen-cooled mercury cadmium telluride (MCT) detector. An indium coating was applied to the fibres to remove cladding modes. Results of attenuation measurement are given in Table 2. When the interstitials holes are collapsed, the losses are greater than 20 dB/m for all the fibres for each wavelength measured. When the interstitials holes are opened, the transmission is significantly improved. For the GeSbS PCF, the attenuation coefficient is 3 dB/m at 1.55 μm and 4.5 dB/m at 3.39 μm. For the AsSe PCF, the loss is 5 dB/m at 1.55 μm and for TAS, it is 9 dB/m at 3.39 μm and 6 dB/m at 9.3 μm.

4. Discussion

Compared to the intrinsic material losses, the transmission measurements show an excess loss of around 20 dB/m for PCF sections with no interstitial holes. However, when the interstitials holes are present, excess losses is reduced to a few dB/m for the three compositions of chalcogenide glass studied. These results indicate that the excess losses are related to the interface between the capillaries. To validate this assumption, we applied 100 mbar of negative pressure to the interstitials holes during the jacketing operation for the GeSbS glass. This value of pressure is enough to perfectly collapse the jacket tube on the microstructure and to partially collapse the interstitials holes. One of the advantages of this glass is its transparency in the visible spectral region. A section of several mms thickness of this perform was then observed using an optical microscope. **Figure 4** shows a superposition of several pictures of the centre of the GeSbS pre-form. A great number of bubbles appear at the capillary interfaces causing significant scattering loss. We believe that the higher the level of negative pressure for a given temperature the higher the number of bubbles which are present. On the other hand, we observe a colour contrast at the capillary interfaces that suggests a change in the refractive index leading to excess loss. At the present time, we do not know the precise nature of this contrast. It may be crystals, very small bubbles or volatile material deposition. We think the same drawbacks happen for the AsSe and TAS glasses. For these two glasses, any observation of the bubbles and index contrast at interfaces in visible spectral region is not possible due to the electronic edge absorption. However, the transmission behaviour is the same for the three compositions glasses studied when the interstitials holes are opened or closed.

The reduction in loss when the interstitial holes are opened is explained by a reduction in the surface area of direct contact between capillaries and in the reduction of the overlap between

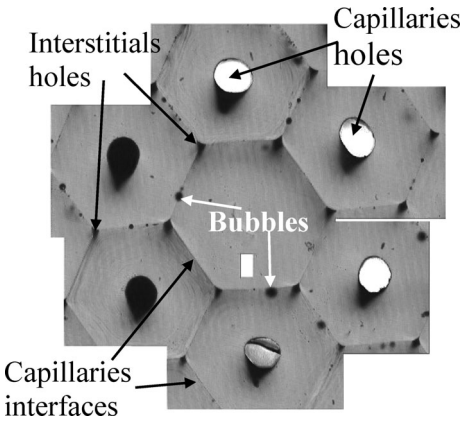

Fig. 4. Cross section of GeSbS preform: Interface problems.

the electric field and the region of the glass interface (the interstitial holes provide supplementary optical confinement). The guided mode therefore encounters a smaller area of glass-glass interface with a consequential reduction in scattering loss. As can be seen from Table 2, the fibre losses are still a few dB/m greater than the intrinsic material losses because a small fraction of the electric field overlaps the glass interfaces. Numerical modelling would allow an optimised PCF design to minimize this overlapping.

5. Conclusion

We have realized photonic crystal fibres with three different compositions of chalcogenide (GeSbS, AsSe and TAS) glass. The "Stack and Draw" technique was used to make the fibre preforms. Using a differential pressurisation technique during the fibre drawing process, we have shown that the presence of interstitials holes greatly improves the transmission of chalcogenide glasses PCFs. For the GeSbS and AsSe PCFs, the best transmission was respectively 3 dB/m and 5 dB/m at 1.55 μm. For the TeAsSe PCF, the best transmission was 6 dB/m at 9.3 μm. However, when the interstitials holes were collapsed, the transmission of all the PCFs was greater than 20 dB/m. We have demonstrated that excess losses are related to the glass interface region. On a GeSbS perform cross-section of a few mm, we observed the presence of a great number of bubbles and an induced refractive index variation at the glass interface region causing significant scattering losses. Parameters of temperature and depression have a significant influence on formation of theses bubbles.

Further work will involve detailed investigation of this interface problem. Firstly, we think the applied depression and draw temperature could be adjusted to limit bubble formation. Secondly, calculations could help to diminish the overlap between the electric field and the interface glass region.

Acknowledgements This work was financially supported by the Agence Nationale pour la Recherche (FUTUR project) and the Délégation Générale pour l'Armement (grant N°0734031004707565).

References

1) F. Smektala, C. Quemard, V. Couderc and A. Barthélémy, *J. Non-Cryst. Solids*, **274**, 232–237 (2000).
2) G. Boudebs, F. Sanchez, J. Troles and F. Smektala, *Opt. Comm.*, **199**, 425–433 (2001).
3) M. Asobe, T. Kanamori, K. Naganuma, H. Itoh and T. Kaino, *J. Appl. Phys.*, **77**, 5518 (1995).
4) H. Nasu, K. Kubodera, H. Kobayashi, M. Nakamura and K. Kamiya, *J. Am. Ceram. Soc.*, **4**, 1794 (1990).
5) T. Arai, M. Kikuchi, M. Saito and M. Takizawa, *J. Appl. Phys.*, **63**, 4359 (1988).
6) E. Papagiakoumou, D. N. Papadopoulos and A. A. Serafetinides, *Opt. Comm.*, **276**, 80–86 (2007).
7) K. Michel, B. Bureau, C. Boussard-Plédel, T. Jouan, J. L. Adam, K. Staubmann and T. Baumann, *Sens. Act. B*, **101**, 252–254 (2004).
8) P. Houizot, C. Boussard-Plédel, A. J. Faber, L. K. Cheng, B. Bureau, P. A. Van Nijnatten, W. L. M. Gielesen, J. Pereiro do Carmo and J. Lucas, *Opt. Exp.*, **19**, 12529–12538 (2007).
9) J. S. Sanghera, L. B. Shaw and I. D. Aggarwal, *Comptes rendus Chimie*, **5**, 873–883 (2002).
10) R. E. Slusher, G. Lenz, J. Hodelin, J. Sanghera, L. B. Shaw and I. D. Aggarwal, *J. Opt. Soc. Am. B*, **21**, 1146–1155 (2004).
11) K. S. Abedin, *Opt. Lett.*, **31**, 1615–1617 (2006).
12) L. B. Fu, M. Rochette, V. G. Ta'eed, D. J. Moss and B. J. Eggleton, *Opt. Express*, **13**, 7637–7644 (2005).
13) D. P. Wei, T. V. Galstian, I. V. Smolnikov, V. G. Plotnichenko and A. Zohrabyan, *Opt. Express*, **13**, 2439–2443 (2005).
14) V. G. Ta'eed, M. R. E. Lamont, D. J. Moss, B. J. Eggleton, D. Y. Choi, S. Madden and B. Luther-Davies, *Opt. Express*, **14**, 11242–11247 (2006).
15) M. Asobe, T. Ohara, I. Yokohama and T. Kaino, *Electron. Lett.*, **32**, 1396 (1996).
16) J. Troles, F. Smektala, G. Boudebs, A. Monteil, B. Bureau and J. Lucas, *Opt. Mat.*, **25**, 231–237 (2004).
17) M. F. Churbanov, I. V. Scripachev, V. S. Shiryaev, V. G. Plotnichenko, S. V. Smetanin, E. B. Kryukova, Y. N. Pyrkov and B. I. Glagan, *J. Non-Cryst. Solids*, **326&327**, 301–305 (2003).
18) J. Kobelke, J. Kirshof, M. Scheffer and A. Schwuchov, *J. Non-Cryst. Solids*, **255&256**, 226–231 (1999).
19) T. A. Birks, J. C. Knight and P. St. J. Russel, *Opt. Lett.*, **22**, 961–963 (1997).
20) T. M. Monro, Y. D. West, D. W. Hewak, N. G. R. Broderick and D. J. Richardson, *Electron. Lett.*, **36**, 1998–2000 (2000).
21) J. Le Person, F. Smektala, L. brilland, T. Chartier, T. Jouan, J. Troles and D. Bosc, *Mat. Res. Bull.*, **41**, 1303–1309 (2006).
22) L. Brilland, F. Smektala, G. Renversez, T. Chartier, J. Troles, T. N. Nguyen, N. Traynor and A. Monteville, *Opt. Express*, **14**, 1280–1285 (2006).
23) L. B. Shaw, P. A. Thielen, F. H. Kunk, V. Q. Nguyen, J. S. Sanghera and I. D. Aggarwal, *Advanced Solid State Photonics*, **98** OSA proceedings, 864–868 (2005).

Laurent Brilland was born in 1971. He received the Ph D degree in physics in 2000. In the years 1998-2002, he worked on the processing of writing Bragg Gratings on optical fiber at the research department of Highwave Optical Technologies. He has developed solutions to produce gain flattening filters. Since 2004, he joined PERFOS where he is currently working on the realization of chalcogenide microstructured fibers. He has strong research links with colleagues of the Equipe Verres and Ceramiques from Rennes.